

ParaGlyder: Probe-driven Interactive Visual Analysis for Multiparametric Medical Imaging Data

Eric Mörth^{1,2}[0000-0003-1625-0146], Ingfrid S. Haldorsen^{2,3}[0000-0001-9313-7564],
Stefan Bruckner^{1,2}[0000-0002-0885-8402], and Noeska N.
Smit^{1,2}[0000-0002-3719-4625]

¹ Department of Informatics, University of Bergen, Norway

² Mohn Medical Imaging and Visualization Centre,
Haukeland University Hospital, Norway

³ Department of Clinical Medicine, University of Bergen, Norway

Abstract. Multiparametric imaging in cancer has been shown to be useful for tumor detection and may also depict functional tumor characteristics relevant for clinical phenotypes. However, when confronted with datasets consisting of multiple values per voxel, traditional reading of the imaging series fails to capture complicated patterns. These patterns of potentially important imaging properties of the parameter space may be critical for the analysis, but standard approaches do not deliver sufficient details. Therefore, in this paper, we present an approach that aims to enable the exploration and analysis of such multiparametric studies using an interactive visual analysis application to remedy the trade-offs between details in the value domain and in spatial resolution. This may aid in the discrimination between healthy and cancerous tissue and potentially highlight metastases that evolved from the primary tumor. We conducted an evaluation with eleven domain experts from different fields of research to confirm the utility of our approach.

Keywords: Medical Visualization · Visual Analysis · Multiparametric Medical Imaging Data

1 Introduction

Multiparametric medical imaging scans are commonly used in screening procedures and in targeted diagnostics. Basing decisions on the analysis of these datasets is not an easy task and often involves visual inspection of different juxtaposed representations [6]. Multiparametric datasets are generated in medical imaging by, e.g., Magnetic Resonance Imaging (MRI) scanners, by varying acquisition parameters resulting in imaging data with varying contrasts. In the analysis of medical imaging data, the main task is usually to identify discernible patterns to distinguish pathologic from healthy tissue, and identify, e.g., malignant tumors. The identification of metastases, likely to share characteristic imaging properties with the primary tumor, may be difficult to spot only using one modality, although identifying them at primary diagnostic work-up is essential to develop more tailored and targeted treatment strategies in various cancers. In order to improve the workflow of tumor diagnosis and metastases identification, we have developed a tool for analyzing multiparametric medical

imaging data together with gynecological cancer, machine learning and neurological cancer research experts. By employing different views displaying multiparametric data at different levels of detail, we can present imaging data without having to visually compare several modalities in side-by-side views. We enable highlighting of target structures, based on multiparametric similarity, which was not possible before. Medical experts are used to working with 2D slice views. Overlaying multiparametric data on top of these views produces insights which are easy for them to put into a spatial context. Showing multiparametric images in one view reduces the cognitive load and allows the medical experts to see the relevant information at a glance. Our main contributions are the following: (1) We present visualizations that remedy the trade-offs between revealing details in the multiparametric value domain and spatial resolution by introducing a multiparametric star glyph map-based visualization. (2) We present an interactive analysis application primarily targeting cancer imaging, as well as additional workflows in different application areas. (3) We evaluate our system with eleven experts using the System Usability Scale (SUS) [3] and a qualitative evaluation to demonstrate the utility of our approach.

2 Medical Background

Modern imaging techniques are routinely used at many centers in the preoperative diagnostic work-up in endometrial cancer. Imaging markers derived from these advanced MRI techniques have been shown to be linked to endometrial cancer subtype and stage [6,11,10,9,2]. According to previous findings, low tumor blood flow and a low rate constant for contrast agent intravasation, meaning the backflow of injected contrast into the close vessels, based on dynamic contrast-enhanced (DCE)-MRI, are associated with high-risk histologic subtypes and poor prognosis. Gathering information from parametric maps based on DCE-MRI is usually done using juxtaposed images of the same slice in the different modalities. These maps are derived from a single dynamic acquisition and are therefore co-registered by nature. Examining the images involves comparing the images mentally or by using a manually placed region of interest (ROI). If advanced imaging methods can be utilized to validly predict the aggressiveness of a tumor, this could lead to better risk-stratified treatment algorithms that may be beneficial for the patients. Less invasive treatment regimens may then be given in low-risk patients, and the more invasive treatments can be reserved for high-risk patients in whom the expected survival benefit justifies the increased side effects.

3 Related Work

Lawonn et al. [16] provide an extensive overview of different visualization techniques for multimodal medical imaging datasets. Gleicher et al. [8] introduced a taxonomy of visual comparison approaches and surveyed existing methods according to it. Friendly et al. [7] proposed radial boxplots, as a means to visualize data variations. Ropinski et al. [22] provide a thorough overview of different glyph-based visualization techniques in the field of multivariate medical data visualization. Wickham et al. [27] introduced a visualization technique called glyph maps. Opach et al. [20] described that the effectiveness of polyline versus

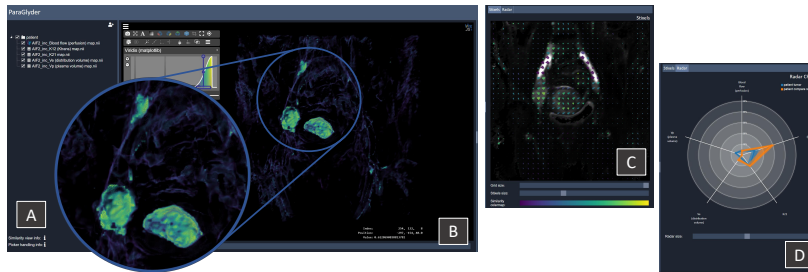


Fig. 1. The ParaGlyder prototype application, featuring a subject overview (A), central view (B), Stixels view (C), and radial boxplot view (D).

star glyphs is task-dependent. The effective combination of star glyphs presenting non-spatial data and geospatial data has been demonstrated by Friendly et al. [7] and more recently by Jäckle et al. [12]. In contrast to this, we use star glyphs to present an abstract version of multiparametric spatial data on top of spatial data. Smit et al. [24] presented a method to spatially query data by placing a sphere in a 3D view, and interaction techniques to effectively place spheres in volume renderings [25]. Bruckner et al. [4] introduced a probing tool for enabling visual queries. Mlejnek et al. [18] presented interactive glyphs for probing tissue characteristics in medical data. In contrast to these approaches, we provide a probing interaction that acts like a digital biopsy of our multiparametric medical imaging datasets. More closely related to our approach, Stoppel et al. [26] used small multiples to visualize spatio-temporal data in a spatial context. Malik et al. [17] introduced a comparative visualization technique that visualizes up to five modalities together in one view. Jönsson et al. [13] presented a visual environment for hypothesis generation using spatial and abstract data. In contrast to these related publications, our approach enables the exploration and analysis of multiparametric medical imaging datasets of more than five modalities. We provide targeted functionality for the analysis of pathology, which allow for inspection of the multiparametric imaging data in linked spatial and non-spatial data visualizations.

4 Requirement Analysis

Following the nested model for visualization design by Munzner [19], we characterized the problem domain. To meet the requirements and the demands of the target audience, we consulted experts in gynecological cancer imaging, neurological imaging, and machine learning. We identified application related challenges they face in their research practice. Cancer imaging is performed to assess tumors and metastases, in gynecological cancer imaging in the pelvic area and for neurological imaging in the brain. Cancerous tissue is discernible because it differs from its surrounding healthy tissue. Besides analysis of the extent and size of the tumor, analyzing different sub-regions within a tumor may be of interest. Finding abdominal lymph node metastases is a challenging task, as the metastases have variable size, ranging from a few millimeters to sizes exceeding the primary tumor. Metastases often share some of the characteristic imaging features of the primary tumor. Based on our analysis we present the following requirements for our interactive analysis application:

- R1: Visual analysis of multiparametric imaging data in a single view
- R2: Multiparametric inhomogeneity analysis
- R3: Comparing regions within the multiparametric imaging data
- R4: Comparing multiparametric imaging data of multiple subjects
- R5: Multiparametric similarity analysis based on a digital biopsy
- R6: Interactive parameter selection for automatic multiparametric segmentation tasks

When satisfying these requirements, we support gynecological imaging researchers, neurological imaging experts and machine learning experts in their research or clinical routine with the ultimate goal of improving patient care by providing better diagnostic tools that can guide tailored and individual treatment strategies.

5 ParaGlyder

In this section, we present our visualization and interaction design decisions based on the requirement analysis. In Figure 2, we present the different components of our method and their interplay. Our design combines spatial and non-spatial visualizations, linked by a view combining a non-spatial visualization in spatial context. Our approach consists of several visualization and interaction methods for the interactive analysis of multiparametric data described in the following.

5.1 Data Processing

Our method relies on multidimensional co-registered volumetric data. Our gynecological cancer experts already deliver co-registered volumes due to the nature of the data source. Co-registration is therefore not part of our application but may be performed by using state of the art applications such as Elastix [14]. Standard MRI imaging data cannot be converted to physical units and therefore is highly dependent on the scanner and sequences employed. In order to allow for comparison normalization is required. In our application, we perform two types of normalization. When we use a slice view, we normalize the data of the slice using a min-max normalization of the selected slice. In the 3D volume visualization, we normalize the whole volume by using the min-max value of the volume. This results in the most appropriate normalization based on the tasks the visualizations support.

5.2 The Stixels View

Based on requirement R1, the goal is to raise the level of detail in the value domain but still keep the details in the spatial resolution. To facilitate this, we

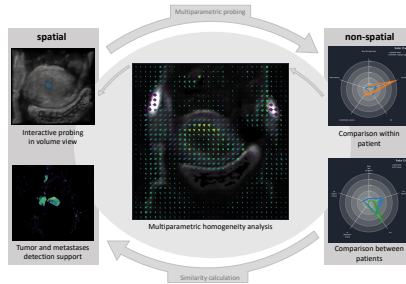


Fig. 2. The ParaGlyder application combines spatial (volumetric view) and non-spatial (radial boxplot) visualization to enable multiparametric analysis and exploration. In between, the Stixels view depicts a combination of both.

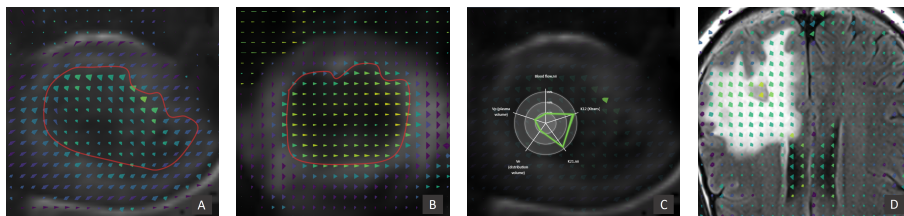


Fig. 3. The Stixels view reveals an inhomogeneous tumor in one subject (a) and a more homogeneous tumor in another subject (b). The outline in red shows the tumor extent for illustration purposes. A tooltip provides details on demand in a radial boxplot (c). The Stixels view reveals oedema in the brain after surgery (d).

employ a glyph map approach, presented in the middle of Figure 2, which is called the Stixels (**Star glyph pixels**) view. The glyph map is based on a regular grid which is overlaid on a 2D view of a slice. For every grid cell, we calculate statistics of the multiparametric medical imaging data. The star glyphs are then created by summarizing the statistics within each of the cells. The grid size and the star glyph size can be adapted, depending on the granularity of the structure of interest. By cropping the slice view to a region of interest, the glyph maps also adapt to the selection and allows for an even more detailed view of the selected structures. We use star glyphs instead of polyline-based glyphs since according to Opach et al. [20] star glyphs are a better choice for finding differences. For the star glyph design, we display the average value of each parameter within the grid cell on the axes. The area described by connecting these points forms a glyph which describes the relation of average parameters within the cell. When designing a star glyph, a homogeneous shape is favorable [21,15]. Therefore, the order in which the parameters are presented is adjustable. While even more information could be encoded on the axes of the star glyph, we opted for a design that is easier to interpret and presents all necessary information at a glance to prevent a steep learning curve. The star glyph map provides an overview which allows the user to identify the tumor since the tissue differs from healthy tissue in the multiparametric dimensions. In addition, the inhomogeneity of the tumor can be analyzed. When spotting interesting parts of the tumor, a closer investigation of the area using the interactive probing can be employed.

5.3 3D Probing Visualization

Requirements R3 and R4 support analyzing different parts of the tumor independently, enabling identification of tumor patterns. Probing spheres deliver detailed information from data within selected regions. Regions of interest can be specified by using multiple probing spheres. This enables a comparison of different regions within the imaging data for a single patient, e.g., healthy tissue and cancerous tissue. All voxels from all parameters within the spheres can be used in the statistical analysis, like the approach used for the star glyph map. For the visual encoding of the probed regions a radial boxplot is used. It shows the user the summary statistics for selected regions of interest at a glance. Comparison is enabled by the superposition of multiple radial boxplots. Radial boxplots are favorable because they align with the use of star glyphs in the Stixels view and represent a more detailed view of selected areas. Differences and similarities

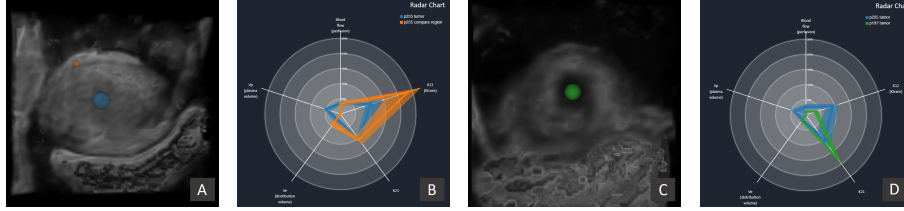


Fig. 4. Volume probing using two different probing spheres (a) results in live updates to the radial boxplot view (b). Probing interaction within another subject (c) results in a radial boxplot comparing data across subjects (d).

over all modalities can be analyzed by placing multiple spheres either within the data of a single patient or multiple patients. To establish visual correspondence between the probing spheres and radial boxplots, both the spheres and boxplot share the same color hue. Interactive probing can be used to define a multiparametric pattern which describes different tumor characteristics based only on imaging data and may also be found in other patients suffering from a similar tumor type.

5.4 Interaction

To support requirements R3 and R4 various interaction methods are provided. The placement of the probing sphere can be performed either in 2D images or in 3D volumes. The size of the sphere can be adapted to fit the scale of the region of interest and the sphere can be placed freely. The quickest option is the free placement where the sphere is placed according to the intersection of a ray going from the screen position, where the mouse is located, towards the volume based on the closest visible point in the volume. In addition to this quick initial placement of the sphere, we introduce a mode where the sphere can only be translated within the current X-Y plane the sphere is located at. Another option only adapts the depth of the sphere along the Z-axis. When using a 2D view, it may occur that the probing sphere is behind the current slice and thus occluded. To remedy this, we provide an option to snap the sphere back to the slice. To support working with brain data, placing a sphere that is automatically mirrored to the other hemisphere is also possible.

5.5 Similarity Visualization

Requirements R5 and R6 state that a similarity analysis and an interactive parameter selection is beneficial in tumor analysis. Analyzing the tumor extent and possible metastases in surrounding tissue is a typical task for radiologists. In addition, segmentation of tumors is an active field of machine learning research, where some algorithms require feature selection. To support these tasks, we employ the multiparametric contents of a probed area in a similarity function. We decided to use the Euclidean distance over all dimensions because they are equally important. When applying this function to each multi-parametric voxel in the volume, we derive a new volume consisting of similarity values between 0 and 1 which can be displayed with an appropriate transfer function. A transfer function that highlights regions of high similarity through color and

opacity enables users to identify structures such as tumors and possible metastases and enables a visual clustering with soft boundaries. Metastases which share the same imaging properties as the primary tumor are highlighted using direct volume rendering. Editing the transfer function enables the user to explore the inhomogeneity (R2) and the extent of different parts of the tumor. In addition, this similarity function-based visual encoding is also applied to the star glyph map. The fact that the similarity is based on the user-selected parameters enables the user to perform interactive feature selection (R6).

6 Results

The ParaGlyder application is depicted in Figure 1 and consists of a center view (Figure 1B), which provides common spatial visualization features, such as a 3D view, 2D slice-based views, cropping, and transfer function editing, and a probing functionality. Next to the main view, the Stixels view is located (Figure 1C), which consists of a 2D slice view and an overlaid glyph map consisting of star glyphs. The last view is the probing view, component D in Figure 1. It consists of a radial boxplot based on probing sphere input. We analyzed different datasets of endometrial cancer patients, provided by one of our co-authors, as well as a brain tumor dataset publicly available and provided by Schmainda and Prah [23] via the Cancer Imaging Archive (TCIA) [5]. The endometrial cancer dataset comprises standard multiparametric MR sequences and derived parameter maps visualizing physical parameters, e.g., blood flow and plasma volume. The data is co-registered due to its origin. For the brain tumor and inflammation data, we have access to the standard parameters acquired in multiparametric MR, such as T1-, T2- and diffusion-weighted images.

6.1 Tumor Detection and Multiparametric Homogeneity Assessment

To detect tumors and assess their multiparametric homogeneity, the Stixels view is used. The user selects the slice and the parameter to show. A detailed view of individual Stixels is presented when the user hovers the mouse over the specific Stixel. A detailed tooltip is shown, visualized in Figure 3c. In order to support region of interest (ROI) selection, we employ volumetric cropping to select an appropriate Stixel window. The grid of the Stixels adapts accordingly and then probes smaller regions determined by the ROI. When placing a probing sphere, the Stixels are colored by the multiparametric similarity, measured based on Euclidean distance, using the Viridis colormap. The similarity Stixels view, visible in Figures 3a and 3b, additionally reveals the inhomogeneity of the tumor. The red line marks the outline of the tumor and the color and shape variations of the star glyphs represents the inhomogeneity within the primary tumor. In Figure 3a, a tumor with a high degree of inhomogeneity is visible, while Figure 3b reveals a more homogeneous tumor. The inhomogeneity analysis enables the user to spot distinct parts within the tumor, e.g., a necrotic core and allows for further analysis of these specific parts in detail.

6.2 Region Comparison for Tumor Characteristic Assessment

Probing spheres are used to analyze different parts within one patient or across multiple patients. This probing interaction is conceptually similar to a digital

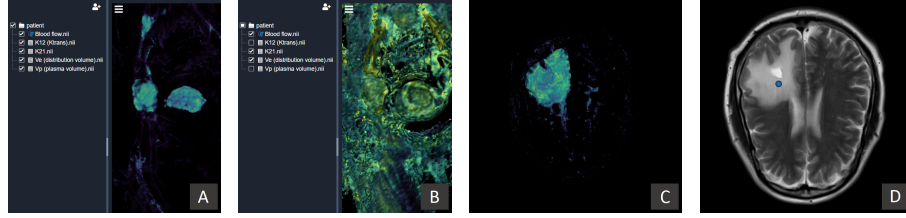


Fig. 5. The similarity view highlighting the uterine primary tumor in the center and two metastatic lymph nodes (a). When an insufficient number of dimensions is selected, the similarity view fails to capture the tumor and metastases (b). The similarity view captures brain inflammation (c), while simple thresholding on one modality would capture the skull as well.

biopsy. The result of the probing interaction is a radial boxplot, visible in component D in Figure 1. Figure 4a showcases placement of two spheres for a single subject, while Figure 4b shows a sphere placed to compare regions across subjects. The radial boxplot is shown in Figure 4b and 4d. On each axis, the median value is presented as a dot, and these dots are connected by lines. In addition to the median value, the 25% and the 75% quantile ranges are visible as an overlaid band. This representation allows the user to see the inhomogeneity of the data within the sphere. The maximum values of the axes can be adapted to fit the selected data range. The spheres are used to characterize tumor tissue and to come up with specific signature shapes in the radial boxplot that can be used to classify the imaging data of new patients. The interaction responsiveness is ensured by providing a real-time update of the radar chart with the probed values of the volumetric multiparametric imaging data while the sphere is moved interactively through the volume.

6.3 Similarity Visualization for Metastases Detection and Feature Selection

The similarity view, visible in Figure 1B and Figure 5, visualizes the extent of a tumor and potential nearby metastases. Figure 5(a) shows the similarity volume when using all multiparametric images and Figure 5(b) shows the similarity volume with only three out of five of the multiparametric images. The Figure shows that the three selected images do not contain enough information to segment the tumor and the metastases. The colored Stixels are presented in Figure 3c. For both approaches the Viridis colormap is chosen as a transfer function, where opacity is mapped to similarity, i.e., the visibility of regions that differ from the current selection is reduced. In component B of Figure 1, the similarity view of parameter maps of a patient with endometrial cancer is visible. This similarity analysis enables a clear and distinct visualization of the tumor (the lower right structure in the inset), by placing a probing sphere inside the tumor tissue. Due to their multiparametric similarity, metastases in the lymphatic system (structures to the left and above the primary tumor) are also highlighted. When analyzing only one of the multiparametric images at a time the detection of metastases is much more difficult because they are not clearly visible. When probing inflammatory data within the brain, the similarity view provides a quick

segmentation of inflamed tissue. The segmentation does not include the bone as a standard thresholding operation based on T2 Flair data only would, visualized in Figure 5(c) and Figure 5(d). This demonstrates that the multiparametric similarity function facilitates a rapid multiparametric segmentation, which could be used in diagnosis or treatment planning, as well as feature analysis as input to automatic segmentation methods in a machine learning context.

Table 1. The response of the experts on a 5-point Likert scale. The values range from 1: Strongly disagree to 5: Strongly agree. Statements marked with a star were rephrased to present the positive form in this table, also the scores have been inverted. On the right end of the table the average value over all experts is presented and in the last row the result of the SUS questionnaire is presented.

Statement	N1	N2	N3	Gy1	Gy2	Gy3	Gy4	Gy5	M1	M2	M3	Avg.
G1 The linked interactions between the center view and the radar chart are well established and intuitive	3	5	4	5	5	5	5	3	5	5	4	4.45
G2 The linked interactions between the analyze view and the Stixel view are well established and intuitive	5	4	4	5	5	5	5	4	5	5	5	4.73
G3 I see myself using the MRI Explorer in the future*	3	5	3	5	5	3	5	5	5	4	4	4.27
G4 I would like to contribute in the future development of the application	5	5	5	5	4	5	3	3	5	4	4	4.45
G5 I can see the application as a part of my daily work routine*	3	5	2	5	4	1	3	5	4	1	1	3.09
G6 The application is more applicable for research than for daily clinical practice	3	4	5	5	4	5	4	3	5	4	2	4.00
G7 The application should be part of the software used in clinical practice*	1	5	1	3	4	3	5	5	4	4	5	3.64
P1 The navigation in 3D is easy to understand and I can place the sphere where I want*	5	4	2	2	5	5	5	4	5	5	5	4.27
P2 The resizing operation of the sphere is easy to understand and to carry out*	4	4	2	5	4	5	5	5	5	4	5	4.36
P3 I can place the sphere anywhere on the plane using the provided keyboard interactions	5	5	3	4	5	4	5	5	5	5	5	4.64
P4 Setting the probing sphere to a specific depth in the volume is intuitive	2	5	2	3	5	4	4	4	5	4	4	3.91
P5 Snapping the probing sphere to the current slice selection is useful	5	4	3	5	5	5	5	4	5	5	3	4.45
P6 The probing interaction is responsive*	3	5	4	5	5	5	5	5	5	5	5	4.73
P7 The automatic update of the Radar chart is beneficial*	5	5	4	5	5	5	4	5	5	5	5	4.82
P8 The radar chart helps me to interpret multimodal data	5	5	5	5	5	5	5	5	5	4	5	4.91
P9 I am confident in interpreting the values that the radar chart presents	3	5	3	4	5	3	4	3	5	5	3	3.91
P10 With the probing functionality, I am able to compare different regions within one subject*	5	5	3	4	5	5	5	5	4	5	4	4.55
P11 The probing function enables me to compare regions between different subjects	3	5	4	5	5	5	4	5	5	3	4	4.36
S1 I understand what the Stixels view shows me and can interpret the star glyphs used.	3	5	4	4	5	3	4	3	5	5	3	4.00
S2 The Stixels view helps me to gather insight of the inhomogeneity of the data*	5	5	3	5	5	5	5	5	5	3	4	4.55
S3 The cropping functionality helps me to focus the Stixel view on the most important region of the subjects data*	1	5	2	5	5	5	5	5	5	5	4	4.27
S4 The different grid sizes help me to first get an overview and add details on demand	5	5	4	5	5	4	5	5	4	5	4	4.64
S5 The tooltip helps me to see more details in the Stixels view when I need them	5	5	4	5	5	5	4	5	5	4	4	4.64
S1 I understand the color coding of the Stixels in terms of similarity*	3	5	4	5	5	5	5	5	5	5	5	4.73
S2 The similarity coloring of the Stixels helps me to adapt my probing selection	3	5	3	5	5	4	4	5	4	5	4	4.27
S3 The similarity volume visualization shows me interesting parts of the volumetric data	5	4	5	5	5	5	5	5	5	5	4	4.82
S4 The similarity view is useful to me and I would like to use it in my work routine/research*	5	5	5	5	5	5	5	5	5	1	4	4.55
Gys1 The application can improve the analysis of the inhomogeneity of gynecological cancer					5	5	5	5				5.00
Gys2 The application can support hypothesis generation for linking parameters with aggressiveness of gynecological cancer					5	5	5	5				5.00
Gys3 I would find this application useful when analyzing patients gynecological cancer MR data*					5	5	5	5				5.00
Gys4 I would like to use this application to explain pathology and treatment to patients					4	5	1	3	3			3.20
Gys5 I would like to use this application to plan a biopsy for analyzing biomarkers of the tumor					X	5	1	3	5			3.50
Gys6 The application is useful for finding metastases*					5	4	2	5				4.20
Gys7 The similarity view shows me the structure of the tumor					5	4	5	5	4			4.60
Gys8 The similarity view shows me the size and structure of possible metastases					5	5	3	5	5			4.60
Ns1 The application helps me to visualize lesions in the brain	5	4	1									3.33
Ns2 Comparing different regions within the brain using the comparison picker is particularly useful for me*	5	5	5									5.00
Ns3 The similarity view helps me to get a better volumetric view of the lesion*	5	5	4									4.67
Ns4 I would like to use this tool to further analyse multiparametric brain imaging data	3	5	4									4.00
Ns5 The interaction with the comparison tool is suitable for brain images	5	5	3									4.33
Ns6 The application helps me see the intensity relations of the different tissue types between modalities*	5	5	5									5.00
Ms1 The application helps me to carry out feature selection prior to applying my machine learning algorithms									4	4	3	3.67
Ms2 I find the similarity view useful to identify which modalities are important for me*									4	4	5	4.33
Ms3 I can imagine using this tool before applying machine learning algorithms*									5	4	4	4.33
Ms4 This application is particularly useful for segmentation based on machine learning									5	4	5	4.67
SUS System usability scale result	97.5	85	40	75	85	80	87.5	80	95	92.5	85	81.75

7 Evaluation

We conducted a qualitative evaluation with eleven experts (6 male, 5 female) from the scientific fields of neurological imaging (N1-3), gynecological cancer imaging (Gy1-5) and machine learning research (M1-3). One expert is co-author and provided us with clinical data of gynecological cancer patients and one expert of each domain (N1, Gy2, M2) was included in the interviews during the development of our application. We were especially interested in validating the effectiveness of the various visualization components and identifying opportunities to make our application more suitable for daily research or even clinical practice.

The individual evaluation started with a short demonstration of the tool, afterwards experts were encouraged to explore and analyze the multiparametric data themselves. They were invited to comment using a think-aloud protocol. The gynecological cancer and machine learning experts worked with endometrial cancer data and the neurological imaging experts with data provided by Schmainda and Prah [23] via the Cancer Imaging Archive (TCIA) [5]. After this phase, which lasted around 30 minutes, we conducted a semi-structured interview with the experts. Finally, a questionnaire consisting of 27 generally applicable statements and 4-8 targeted statements for the different expert groups was conducted. The experts were asked to indicate their level of agreement using a five-point Likert scale. In addition to our targeted evaluation form, we asked the experts to fill out the system usability scale (SUS) provided by Brook et al. [3]. The evaluation results of the eleven participants are shown in Table 1.

We conclude from the results presented in Table 1 that the application is overall valuable for the experts. The probing interaction was rated favorably, two participants would appreciate a guided 3D placement of the probe. All study participants think that the Stixels view helps them to see inhomogeneous regions within the Slice view. The similarity view received the most positive feedback and is potentially useful for all involved experts. The targeted statements demonstrate that the application is applicable different scenarios, albeit for different reasons. The gynecological experts envision that the application could improve the assessment of tumor heterogeneity both in primary tumors and metastases. The SUS scores range from 40 to 97,5, where the second lowest score is 75. On average, the SUS score is 81,75. According to Bangor et al. [1], the score can be interpreted to be between good and excellent.

8 Conclusion and Future Work

We present ParaGlyder, a multiparametric image visualization tool. The tool provides different views for tumor detection, inhomogeneity analysis, feature selection, and diagnosis in multiparametric medical images, by a tight coupling of spatial and non-spatial data visualization techniques. Our tool is based on a combination of star glyph maps and radar charts. A built-in similarity visualization of the volumetric data enables the visualization of, e.g., primary tumor and the corresponding metastases. The qualitative evaluation confirmed the utility of our application for diverse application areas. In the future, we plan to extend our approach to analysis of larger patient cohorts in order to assess whether this visualization tool could aid in the detection of metastases. Furthermore, the application has the potential to unravel patient-specific imaging features that may be linked to specific clinical phenotypes and outcomes, thus representing a promising tool to facilitate more personalized treatment strategies.

References

1. Bangor, A., Kortum, P., Miller, J.: Determining what individual SUS scores mean: Adding an adjective rating scale. *J. Usability Studies* 4(3), 114–123 (May 2009)
2. Berg, A., Fasmer, K.E., Mauland, K.K., Ytre-Hauge, S., Hoivik, E.A., Husby, J.A., Tangen, I.L., Trovik, J., Halle, M.K., Woie, K., Bjørge, L., Bjørnerud, A., Salvesen,

- H.B., Werner, H.M.J., Krakstad, C., Haldorsen, I.S.: Tissue and imaging biomarkers for hypoxia predict poor outcome in endometrial cancer. *Oncotarget* **7**(43), 69844–69856 (2016). <https://doi.org/10.18632/oncotarget.12004>
3. Brooke, J.: SUS-a quick and dirty usability scale. usability evaluation in industry. In: Jordan, P., Thomas, B., McClelland, I., Weerdmeester, B. (eds.) *Usability Evaluation In Industry*, chap. 10, pp. 266–290. CRC Press (2004)
 4. Bruckner, S., Solteszova, V., Gröller, E., Hladuvka, J., Bühler, K., Yu, J., Dickson, B.: Braingazer - visual queries for neurobiology research. *IEEE transactions on visualization and computer graphics* **15**, 1497–504 (11 2009). <https://doi.org/10.1109/TVCG.2009.121>
 5. Clark, K., Vendt, B., Smith, K., Freymann, J., Kirby, J., Koppel, P., Moore, S., Phillips, S., Maffitt, D., Pringle, M., Tarbox, L., Prior, F.: The cancer imaging archive (tcia): Maintaining and operating a public information repository. *Journal of Digital Imaging* **26**(6), 1045–1057 (Dec 2013). <https://doi.org/10.1007/s10278-013-9622-7>
 6. Fasmer, K.E., Bjørnerud, A., Ytre-Hauge, S., Grüner, R., Tangen, I.L., Werner, H.M., Bjørge, L., Salvesen, Ø.O., Trovik, J., Krakstad, C., Haldorsen, I.: Preoperative quantitative dynamic contrast-enhanced mri and diffusion-weighted imaging predict aggressive disease in endometrial cancer. *Acta Radiologica* **59**(8), 1010–1017 (2018). <https://doi.org/10.1177/0284185117740932>
 7. Friendly, M.: A.-M. Guerry’s Moral Statistics of France: Challenges for multivariable spatial analysis. *Statistical Science* **22**(3), 368–399 (2007). <https://doi.org/10.1214/07-STS241>
 8. Gleicher, M., Albers, D., Walker, R., Jusufi, I., Hansen, C.D., Roberts, J.C.: Visual comparison for information visualization. *Information Visualization* **10**(4), 289–309 (2011). <https://doi.org/10.1177/1473871611416549>
 9. Haldorsen, I.S., Stefansson, I., Grüner, R., Husby, J.A., Magnussen, I.J., Werner, H.M.J., Salvesen, Ø.O., Bjørge, L., Trovik, J., Taxt, T., Akslen, L.A., Salvesen, H.B.: Increased microvascular proliferation is negatively correlated to tumour blood flow and is associated with unfavourable outcome in endometrial carcinomas. *British Journal of Cancer* **110**(1), 107–114 (2014). <https://doi.org/10.1038/bjc.2013.694>
 10. Haldorsen, I.S., Grüner, R., Husby, J.A., Magnussen, I.J., Werner, H.M.J., Salvesen, Ø.O., Bjørge, L., Stefansson, I., Akslen, L.A., Trovik, J., Taxt, T., Salvesen, H.B.: Dynamic contrast-enhanced MRI in endometrial carcinoma identifies patients at increased risk of recurrence. *European Radiology* **23**(10), 2916–2925 (Oct 2013). <https://doi.org/10.1007/s00330-013-2901-3>
 11. Haldorsen, I.S., Salvesen, H.B.: What is the best preoperative imaging for endometrial cancer? *Current Oncology Reports* **18**(4), 25 (Feb 2016). <https://doi.org/10.1007/s11912-016-0506-0>
 12. Jäckle, D., Fuchs, J., Keim, D.A.: Star glyph insets for overview preservation of multivariate data. IS and T International Symposium on Electronic Imaging Science and Technology pp. 1–9 (2016). <https://doi.org/10.2352/issn.2470-1173.2016.1.vda-506>
 13. Jönsson, D., Bergström, A., Forsell, C., Simon, R., Engström, M., Ynnerman, A., Hotz, I.: A visual environment for hypothesis formation and reasoning in studies with fMRI and multivariate clinical data. In: Kozlíková, B., Linsen, L., Vázquez, P.P., Lawonn, K., Raidou, R.G. (eds.) *Eurographics Workshop on Visual Computing for Biology and Medicine*. The Eurographics Association (2019). <https://doi.org/10.2312/vcbm.20191232>

14. Klein, S., Staring, M., Murphy, K., Viergever, M.A., Pluim, J.P.W.: Elastix: A toolbox for intensity-based medical image registration. *IEEE Transactions on Medical Imaging* **29**(1), 196–205 (Jan 2010). <https://doi.org/10.1109/TMI.2009.2035616>
15. Klippel, A., Hardisty, F., Weaver, C.: Star plots: How shape characteristics influence classification tasks. *Cartography and Geographic Information Science* **36**(2), 149–163 (2009). <https://doi.org/10.1559/152304009788188808>
16. Lawonn, K., Smit, N., Bühler, K., Preim, B.: A survey on multimodal medical data visualization. *Computer Graphics Forum* **37**(1), 413–438 (2017). <https://doi.org/10.1111/cgf.13306>
17. Malik, M.M., Heinzl, C., Gröller, M.E.: Comparative visualization for parameter studies of dataset series. *IEEE Transactions on Visualization and Computer Graphics* **16**(5), 829–840 (Sep 2010). <https://doi.org/10.1109/TVCG.2010.20>
18. Mlejnek, M., Ermes, P., Vilanova, A., van der Rijt, R., van den Bosch, H., Geritsen, F., Gröller, M.E.: Profile flags: a novel metaphor for probing of t2 maps. In: C. T. Silva, E. Gröller, H.R. (ed.) *Proceedings of IEEE Visualization 2005*. pp. 599–606. IEEE CS (Oct 2005)
19. Munzner, T.: A nested model for visualization design and validation. *IEEE Transactions on Visualization and Computer Graphics* **15**(6), 921–928 (2009)
20. Opach, T., Popelka, S., Dolezalova, J., Rød, J.K.: Star and polyline glyphs in a grid plot and on a map display: which perform better? *Cartography and Geographic Information Science* **45**(5), 400–419 (2018). <https://doi.org/10.1080/15230406.2017.1364169>
21. Peng, W., Ward, M.O., Rundensteiner, E.A.: Clutter reduction in multi-dimensional data visualization using dimension reordering. *Proceedings - IEEE Symposium on Information Visualization, INFO VIS* pp. 89–96 (2004). <https://doi.org/10.1109/INFVIS.2004.15>
22. Ropinski, T., Oeltze, S., Preim, B.: Visual computing in biology and medicine: Survey of glyph-based visualization techniques for spatial multivariate medical data. *Comput. Graph.* **35**(2), 392–401 (Apr 2011). <https://doi.org/10.1016/j.cag.2011.01.011>
23. Schmainda, K., Prah, M.: Data from brain-tumor-progression (2018). <https://doi.org/10.7937/K9/TCIA.2018.15quzvnv>
24. Smit, N.N., Kraima, A.C., Jansma, D., Ruiter, M.C.d., Botha, C.P.: A Unified Representation for the Model-based Visualization of Heterogeneous Anatomy Data. In: Meyer, M., Weinkauff, T. (eds.) *EuroVis - Short Papers*. The Eurographics Association (2012). <https://doi.org/10.2312/PE/EuroVisShort/EuroVisShort2012/085-089>
25. Smit, N.N., Haneveld, B.K., Staring, M., Eisemann, E., Botha, C.P., Vilanova, A.: RegistrationShop: An Interactive 3D Medical Volume Registration System. In: Viola, I., Buehler, K., Ropinski, T. (eds.) *Eurographics Workshop on Visual Computing for Biology and Medicine*. The Eurographics Association (2014). <https://doi.org/10.2312/vcbm.20141193>
26. Stoppel, S., Hodneland, E., Hauser, H., Bruckner, S.: Graxels: Information rich primitives for the visualization of time-dependent spatial data. In: *Eurographics Workshop on Visual Computing for Biology and Medicine*. pp. 183–192 (sep 2016). <https://doi.org/10.2312/vcbm.20161286>
27. Wickham, H., Hofmann, H., Wickham, C., Cook, D.: Glyph-maps for visually exploring temporal patterns in climate data and models. *Environmetrics* **23**(5), 382–393 (2012). <https://doi.org/10.1002/env.2152>